Laboratory Investigation (2008) 88, 664–681

Helicobacter pylori invades the gastric mucosa and translocates to the gastric lymph nodes

Takashi Ito[1], Daisuke Kobayashi[1], Keisuke Uchida[2], Tamiko Takemura[3], Sakae Nagaoka[4], Intetsu Kobayashi[5], Tetsuji Yokoyama[6], Ikuo Ishige[7], Yuki Ishige[1], Noriko Ishida[2], Asuka Furukawa[1], Hiroe Muraoka[5], Satoshi Ikeda[1], Masaki Sekine[2], Noboru Ando[2], Yoshimi Suzuki[1], Tetsuo Yamada[1], Takashige Suzuki[1] and Yoshinobu Eishi[1,2]

Helicobacter pylori has been considered to be non-invasive and to rarely infiltrate the gastric mucosa, even though there is an active Th1 immune response in the lamina propria of the *H. pylori*-infected stomach. To elucidate whether *H. pylori* invades the lamina propria and translocates to the gastric lymph nodes, we examined *H. pylori* in formalin-fixed and paraffin-embedded tissue sections of stomach and gastric lymph nodes obtained from 51 cancer patients using real-time PCR and immunohistochemistry (IHC) with a novel anti-*H. pylori* monoclonal antibody that recognizes lipopolysaccharides. Fresh gastric lymph nodes were used to culture for *H. pylori*. In 46 patients with *H. pylori* in the stomach, the bacterium was found in the lymph nodes from 21 patients by culture, 37 patients by PCR, and 29 patients by IHC. *H. pylori* captured by macrophages was found in the lamina propria of 39 patients. In the lymph nodes, the bacterium was found in many macrophages and a few interdigitating dendritic cells at the paracortical areas. *H. pylori* was also found in the intracellular canaliculi of parietal cells in 21 patients, but intracytoplasmic invasion into gastric epithelial cells was not identified. When compared to the commercially available anti-*H. pylori* antibodies, the novel antibody showed the highest sensitivity to detect *H. pylori*-positive macrophages, whereas no difference was found for *H. pylori* in the mucous layer. The *H. pylori*-positive macrophages in the lamina propria correlated with chronic gastritis as well as translocation of such cells to the lymph nodes. These results suggest that *H. pylori*-induced gastric epithelial damage allows the bacteria to invade the lamina propria and translocate to the gastric lymph nodes, which may chronically stimulate the immune system. The bacteria captured by macrophages, whether remaining alive or not, may contribute to the induction and development of *H. pylori*-induced chronic gastritis.

Laboratory Investigation (2008) **88,** 664–681; doi:10.1038/labinvest.2008.33; published online 12 May 2008

KEYWORDS: bacterial invasion; bacterial translocation; culture; gastritis; immunohistochemistry; real-time PCR

Helicobacter pylori infection is implicated in the pathogenesis of a number of digestive tract disorders, such as chronic active gastritis, peptic ulceration, gastric cancer, and mucosa-associated lymphoid tissue lymphoma.[1] Chronic active gastritis is the primary disorder that results from *H. pylori* colonization. This condition can potentially develop in all *H. pylori*-positive subjects.[2] *H. pylori*-induced ulcer disease, gastric cancer, and lymphoma are all complications of this chronic inflammation.[3]

H. pylori-induced active gastritis is triggered primarily by *H. pylori* attaching to epithelial cells.[4] Once attached to the gastric epithelial cells, *H. pylori* injects effector molecules into gastric epithelial cells or the lamina propria via a type IV secretion system.[5] The CagA effector molecule activates the epithelial expression of interleukin (IL)-8, which causes polymorphonuclear (PMN) cell infiltration.[6] Another effector molecule, VacA, causes massive vacuolar degeneration of epithelial cells *in vitro* and epithelial erosion *in vivo*.[7]

The development of *H. pylori*-induced chronic gastritis depends predominantly on the Th1-type T-cell response.[8,9] The accumulation of *H. pylori*-specific $CD4^+$ T cells in the *H. pylori*-infected human gastric mucosa[10] suggests that $CD4^+$ T-cell-mediated Th1 immune responses have a critical role in the development of *H. pylori*-induced gastritis. Where

[1]Department of Human Pathology, Tokyo Medical and Dental University Graduate School, Tokyo, Japan; [2]Department of Pathology, Tokyo Medical and Dental University Hospital, Tokyo, Japan; [3]Department of Pathology, Japanese Red Cross Medical Center, Tokyo, Japan; [4]Department of Surgery, Japanese Red Cross Medical Center, Tokyo, Japan; [5]Chemotherapy Department, Mitsubishi Chemical Medience, Tokyo, Japan; [6]Department of Technology Assessment and Biostatistics, National Institute of Public Health, Saitama, Japan and [7]Department of Stem Cell Therapy, Institute of Medical Science, University of Tokyo, Tokyo, Japan
Correspondence: Professor Y Eishi, MD, MedScD, PhD, Department of Human Pathology, Tokyo Medical and Dental University, 1-5-45 Yushima, Bunkyo-ku, Tokyo 113-8510, Japan. E-mail: eishi.path@tmd.ac.jp

Received 18 February 2008; revised 06 March 2008; accepted 06 March 2008

$CD4^+$ T cells are primed by *H. pylori* antigens and how the *H. pylori*-induced chronic inflammation is maintained by T cells, however, are unclear because *H. pylori* appears not to be invasive and rarely infiltrates the gastric mucosa.[11] *H. pylori* is generally observed only in the gastric mucous layer or in the spaces between gastric mucus-secreting cells, and not in the gastric epithelial cells or the lamina propria.[12]

Although in the 1980s investigators emphasized the absence of *H. pylori* within the lamina propria,[13–15] the presence of *H. pylori* within the lamina propria of the human gastric mucosa was described in the 1990s. Both whole *H. pylori* and *H. pylori*-immunopositive material are found in the lamina propria of biopsy specimens from *H. pylori*-positive patients.[16] *H. pylori* surface proteins are also detected within the lamina propria of the gastric antrum from patients with *H. pylori*-associated gastritis.[17] In a study of patients with non-ulcer dysplasia, the presence of whole bacterial cells, mainly the coccoidal form, was described in the tunica propria of the gastric antrum.[18] The invasion of *H. pylori* into the lamina propria was confirmed by immunoelectron microscopy.[19,20]

These observations that *H. pylori* invades the gastric mucosa have not been integrated into the pathogenesis of *H. pylori*-associated gastritis, however, even in recent reviews,[1,3,11] but the presence of *H. pylori* in the lamina propria may be an important factor in the induction and development of gastric inflammation. *H. pylori* invasion of the lamina propria stimulates the mucosal inflammatory cells more intensely than does the bacterium attached to the epithelial cells. *H. pylori* that has invaded the gastric mucosa may translocate to the gastric lymph nodes and chronically stimulate the immune system.

The aim of the present study was to determine whether *H. pylori* invades the gastric mucosa and translocates to the draining lymph nodes. The stomach and gastric lymph nodes removed by surgery for gastric cancer were used for the study. To examine the possible translocation of the bacterium, a fresh gastric lymph node was removed before gastrectomy during surgery and cultured for *H. pylori*. To locate *H. pylori* in the formalin-fixed paraffin-embedded tissue sections, a novel monoclonal antibody (mAb) specific to the bacterium was developed, and the results of immunohistochemistry (IHC) with the antibody were compared to those with the commercially available anti-*H. pylori* polyclonal antibody (pAb) and mAb. Real-time PCR was used to detect *H. pylori* DNA in the histologic sections and the results were compared to those obtained with IHC.

MATERIALS AND METHODS

Patients

A total of 51 consecutive patients with gastric cancer at the Japanese Red Cross Medical Center undergoing gastrectomy and lymph node dissection between April 2001 and April 2003 were enrolled in the study. Clinicopathologic profiles of the patients according to the classification of the World Health Organization[21] are shown in Table 1. Written informed consent was obtained from all patients after explanation of the purpose of this study. The Ethics Committee of the medical center approved the study.

Sampling

One of the gastric lymph nodes along the lesser curvature, the no. 3 lymph nodes according to the Japanese classification of gastric carcinoma,[22] without metastasis was dissected before gastrectomy during surgery and hemisected with a sterile knife under sterile conditions. Half of the lymph node was processed for immediate diagnosis with frozen sections to confirm the absence of cancer metastasis. The other half of the tissue was placed in a Seed Tube 'HP' (Eiken Chemical Co. Ltd, Tokyo, Japan), and transported at 4°C to a laboratory (Mitsubishi Chemical Medience, Tokyo, Japan) where the tissues were cultured within 24 h after the sampling. The stomach and gastric lymph nodes were fixed in 10% buffered formalin for 1 day and processed for routine pathologic examination. Paraffin-embedded tissue (3–4 cm in length) blocks of the stomach taken from the gastric body and antrum that were free from cancer spread were used for the study. Paraffin blocks that included all of the regional lymph nodes along the lesser curvature (no. 3 lymph nodes) and along the right gastroepiploic vessels (no. 4d lymph nodes) were also used for the study.

Culture

After the lymph node was weighed, the tissue was homogenized and diluted with Hanks' balanced salt solution (Invitrogen Co., CA, USA) and cultured on a selective agar plate (Columbia *H. pylori* agar; Becton Dickinson, MD, USA). The agar plate was incubated for 7 days at 35°C in an incubator (Tabai Espec, Osaka, Japan) in an atmosphere containing 10% CO_2. *H. pylori* was identified by its requirement for a 10% CO_2 atmosphere for growth and its typical morphology, and positive biologic tests (oxidase, catalase, and urease). The value of colony-forming units per gram tissue (CFU/g) was calculated by the number of colonies on the selective agar plate and dilution rate. Samples with one or more CFU/g were designated as having positive culture results.

mAb Production

A novel mAb was developed to locate *H. pylori* on the formalin-fixed and paraffin-embedded tissue sections. mAbs were generated according to the protocol described in a laboratory manual[23] with modifications. BALB/c mice (CLEA Japan Inc., Tokyo, Japan) were immunized with sonicated whole bacterial lysate of *H. pylori* (a combination of strains ATCC 43504, ATCC 43579, and ATCC 43629). Hybridoma cell lines producing anti-*H. pylori* antibodies were checked by enzyme-linked immunosorbent assay (ELISA) with the bacterial antigens used as an immunogen. Hybridomas giving positive results were screened by IHC with formalin-fixed and paraffin-embedded tissue sections of *H. pylori*-infected rat liver as well as human stomach (from patient no. 9) and

Table 1 Clinicopathologic profiles of the patients

Profiles	Number of patients
Age (mean ± s.d.)	61 ± 10 years
Sex	
Men	39
Women	12
Location of the tumor	
Upper third	11
Middle third	22
Lower third	18
Lesser curvature	29
Greater curvature	5
Anterior wall	9
Posterior wall	8
Tumor size	
Small (MD[a] < 3.0 cm)	16
Medium (3.0 cm ≤ MD < 6.0 cm)	16
Large (MD ≥ 6.0 cm)	19
Ulceration of the tumor	
Positive	37
Negative	14
Histologic classification	
Papillary carcinoma	2
Tubular adenocarcinoma	
Well differentiated	6
Moderately differentiated	26
Poorly differentiated	9
Signet ring cell carcinoma	8
Lymphatic invasion	
Positive	35
Negative	16
Venous invasion	
Positive	28
Negative	23
TNM classification	
T1	25
T2	14
T3	11
T4	1
N0	34
N1	10
N2	5
N3	2
M0	48
M1	3
Stage I	33
Stage II	6
Stage III	7
Stage IV	5
No. 3 lymph node metastasis	
Positive	7
Negative	44
No. 4d lymph node metastasis	
Positive	3
Negative	48

The clinicopathologic profiles were coded as dummy variables and used to adjust for their potential confounding effects in the correlation analyses in Tables 5–7.

[a]MD: maximum diameter.

gastric lymph nodes (from patient no. 27) from which a large number of *H. pylori* were cultured. *H. pylori*-infected rat liver was obtained by intravenous infection of 30 mg of heat-killed *H. pylori* to female Sprague–Dawley rats (CLEA Japan Inc.) 3 h before being killed. Finally, the hybridoma producing the antibody that generated the most specific reaction products on the human tissue sections was selected and cloned by two rounds of limiting dilution. A single hybridoma clone was then implanted in the intraperitoneal space of the severe combined immunodeficiency mice (CLEA Japan Inc.). At 1 week before the implantation, these mice were injected with pristane (Sigma-Aldrich Co., MO, USA). At 1 or 2 weeks after the implantation, ascites were collected and used as an undiluted mAb without further purification. The antibody (IgG3, κ) was named TMDU-mAb in the study.

IHC

All samples were examined by IHC, and the results obtained using the TMDU-mAb, the mouse anti-*H. pylori* mAb (clone 4H3.2; Chemicon, CA, USA), and the rabbit anti-*H. pylori* pAb (DAKO, Glostrup, Denmark) were compared. Histologic sections (4 μm thick) were cut from formalin-fixed and paraffin-embedded tissue samples and mounted on Silane-coated slides (Muto Pure Chemicals Co. Ltd., Tokyo, Japan). After the sections were deparaffinized and rehydrated, they were microwaved (Microwave Processor H2850; Energy Beam Sciences Inc., CT, USA) in 10 mM citrate buffer (pH 6.0) for 1 h at 99°C. The sections were then treated with 3% hydrogen peroxide in methanol for 30 min. The sections were first incubated with normal horse serum (Vectastain Universal Elite ABC Kit; Vector Laboratories, CA, USA). Subsequently, the sections were incubated overnight at room temperature with either of the appropriately diluted antibodies (TMDU-mAb 1:8000, Chemicon-mAb 1:2000, and DAKO-pAb 1:1000, respectively) in a humidified chamber. The sections were then incubated for 30 min with biotinylated horse antibody, which recognizes rabbit and mouse IgG (H + L) (Vectastain Universal Elite ABC Kit), followed by 30-min incubation with streptavidin-peroxidase complex (Vectastain Universal Elite ABC Kit), both at room temperature. Before and after each step, the sections were washed in phosphate-buffered saline (PBS) containing 0.25% Tween-20 (T-PBS). The signal was developed as a brown reaction product using peroxidase substrate 3,3′-diaminobenzidine tetrahydrochloride (Histofine Simplestain DAB Solution; Nichirei Bioscience, Tokyo, Japan). All specimens were counterstained with Mayer's hematoxylin. The IHC results were considered to be positive when 10 or more signals or cells with signals were identified in each location of the stomach and lymph nodes.

Immunofluorescence Double Staining

Samples with many *H. pylori*-positive cells from the stomach (from patient nos. 2, 43, 47, 48, and 49) and the gastric lymph nodes (from patient nos. 6, 37, 42, 45, and 48) were

used for immunofluorescence double staining to phenotype the cells with intracellular *H. pylori*, using the antibodies to phagocytes; anti-human CD68 mAb (clone KP1; DAKO) for macrophages, anti-human fascin mAb (clone 55K-2; DAKO) for dendritic cells, and anti-human myeloperoxidase (MPO) pAb (DAKO) for PMN neutrophils. Deparaffinized tissue sections (2 μm thick) were microwaved for 1 h at 99°C. After incubation with normal horse serum, sections were incubated for 30 min at room temperature with the TMDU-mAb and then with the biotinylated secondary antibody as described above. Then the sections were incubated for 30 min at room temperature with fluorescein isothiocyanate-conjugated streptavidin (DAKO) in the dark. After microwaving again for 20 min, the sections were incubated overnight at room temperature with either of the appropriately diluted antibodies (anti-CD68 mAb 1:8000, anti-fascin mAb 1:100, and anti-MPO pAb 1:200). The sections were then incubated for 30 min at room temperature with either the tetramethylrhodamine isothiocyanate-conjugated anti-mouse or anti-rabbit immunoglobulins (DAKO) in the dark. Before and after each step, the sections were washed in T-PBS. Finally, sections were coverslipped with fluorescence mounting medium (DAKO). Stained sections were observed and photographed using a microscope BZ-9000 (Keyence, Osaka, Japan).

Immunoelectron Microscopy

The same samples used in the fluorescence double staining were further analyzed by immunoelectron microscopy. Paraffin sections (6 μm thick) were processed in the same manner as for immunoperoxidase staining until the secondary antibody reaction. Subsequently, sections were

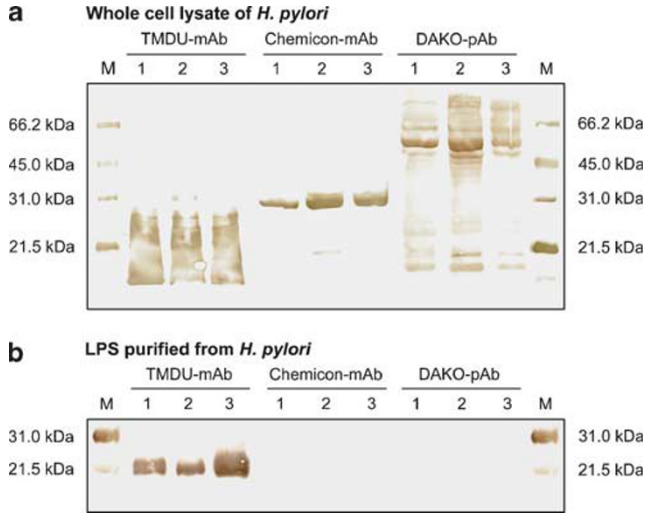

Figure 1 Western blot analysis for the reactivity of the anti-*H. pylori* antibodies. Western blot analysis was performed for the sonicated whole cell lysate (**a**) and purified LPS (**b**) from the three strains of *H. pylori* (lane 1, ATCC 43504; lane 2, ATCC 43579; and lane 3, ATCC 43629). The TMDU-mAb reacted with the *H. pylori* LPS, which was detected by the antibody as a ladder pattern of diffuse bands below the 31.0-kDa size marker (M) on the membrane (**a**), and relatively sharp bands just above the 21.5-kDa size marker on the membrane (**b**). The Chemicon-mAb reacted with a sharp protein band and the DAKO-pAb reacted with multiple protein bands on the membrane (**a**), but neither antibody reacted with the purified LPS on the membrane (**b**).

Table 2 Specificity of the *H. pylori* PCR and the reactivity of the anti-*H. pylori* antibodies

Bacteria	Strain	Results (mean ± s.d.) of the *H. pylori* PCR	Reactivity of the antibodies from TMDU/Chemicon/DAKO by	
			ELISA	Western blot
Helicobacter pylori	ATCC 43504	15 670 ± 2691	+/+/+	+/+/+
Helicobacter pylori	ATCC 43579	14 821 ± 1147	+/+/+	+/+/+
Helicobacter pylori	ATCC 43629	16 192 ± 1988	+/+/+	+/+/+
Helicobacter hepaticus	3B1	41 ± 27	−/−/+	−/−/+
Helicobacter bilis	ATCC 51630	2 ± 5	−/−/−	−/−/−
Campylobacter coli	ATCC 33559	0	−/−/−	−/−/−
Campylobacter jejuni	ATCC 33560	0	−/−/−	−/−/−
Vibrio parahaemolyticus	ATCC 17802	0	−/−/−	−/−/−
Escherichia coli	ATCC 25922	0	−/−/−	−/−/−
Salmonella enteritidis	ATCC 13076	0	−/−/−	−/−/−
Bacteroides fragilis	ATCC 25285	0	−/−/−	−/−/−
Staphylococcus epidermidis	ATCC 12228	0	−/−/−	−/−/−
Streptococcus sanguis	ATCC 10556	0	−/−/−	−/−/−
Mycobacterium tuberculosis	ATCC 27294	0	−/−/−	−/−/−
Propionibacterium acnes	ATCC 6919	0	−/−/−	−/−/−

Table 3 PCR and IHC results from the stomach and gastric lymph nodes and the culture results from the lymph nodes

Patient no.	Stomach					Gastric lymph nodes				Culture (CFU/g)
	PCR		IHC (corpus/antrum)			PCR		IHC (no. 3/no. 4d)		
	Corpus	Antrum	ML[a]	LP[b]	PC[c]	No. 3	No. 4d	Paracortex	Sinus	
H. pylori-negative patients										
29	0	0	−/−	−/−	−/−	0	0	−/−	−/−	0
31	0	0	−/−	−/−	−/−	0	0	−/−	−/−	0
32	0	0	−/−	−/−	−/−	0	0	−/−	−/−	0
36	0	0	−/−	−/−	−/−	0	0	−/−	−/−	0
46	0	0	−/−	−/−	−/−	0	0	−/−	−/−	0
H. pylori-positive patients										
21	147	0	−/−	−/−	−/−	0	0	−/−	−/−	0
3	178	0	−/−	−/−	−/−	0	0	−/−	−/−	0
26	284	0	+/−	+/−	−/−	0	0	−/−	−/−	0
25	370	59	−/−	+/−	−/−	0	0	−/−	−/−	0
18	419	0	+/−	+/−	−/−	0	0	−/−	−/−	120
44	440	2200	+/+	+/+	−/−	240	1040	−/−	−/−	280
17	605	945	+/−	+/+	−/−	71	30	−/−	−/−	0
10	670	262	−/−	+/−	+/−	205	263	−/+	−/+	710
4	775	0	+/−	+/−	+/−	231	47	−/−	−/−	0
16	810	60	−/−	−/−	−/−	138	451	+/−	−/−	600
42	1040	2080	+/−	−/−	−/−	200	400	+/+	+/−	0
50	1040	0	+/−	+/−	−/−	24	0	−/−	−/−	380
30	1520	840	+/−	+/−	+/−	40	0	−/−	−/−	0
27	1770	4130	+/+	+/+	−/−	0	2385	−/+	−/−	1300
39	1800	360	−/−	−/−	−/−	240	0	+/−	−/−	0
1	1820	0	+/−	−/−	−/−	0	0	−/−	−/−	1200
33	3000	0	+/−	+/−	−/−	0	0	−/−	−/−	0
23	3660	870	+/−	+/−	−/−	73	940	+/−	−/−	0
28	4230	796	+/+	+/+	−/−	0	0	−/−	−/−	4400
37	4290	910	+/−	+/−	−/−	2210	109	+/−	−/−	0
22	4780	227	+/−	+/−	+/−	92	53	−/−	−/−	0
14	5050	3750	+/+	+/+	−/−	3270	3850	+/−	−/−	0
15	5100	815	+/−	+/−	−/−	363	0	+/−	−/−	0
24	5750	32	+/−	+/+	+/−	215	0	+/−	−/−	0
20	7100	86 000	+/+	−/−	−/−	418	0	−/−	−/−	330
12	7550	19 200	+/+	+/+	−/−	383	0	−/−	−/−	250
5	12 100	443	+/−	+/−	−/−	0	0	−/−	−/−	0
34	14 400	1400	+/−	+/+	−/−	600	200	+/+	−/−	0
45	15 000	109 000	+/+	+/+	−/−	9520	1840	+/+	−/−	160
13	18 800	20 100	+/+	+/+	−/−	11 900	2900	+/+	−/−	0
7	22 400	16 200	+/+	+/+	+/−	0	1300	−/+	−/−	110
41	23 400	560	+/+	−/+	+/−	40	280	−/+	−/−	0
35	23 400	5760	+/+	+/+	−/+	120	280	+/+	−/−	280
8	25 900	25 400	+/+	+/+	+/−	0	865	−/+	−/−	0
38	29 000	156 000	+/+	+/+	−/+	18 600	3480	+/+	−/−	0
6	43 700	11 000	+/+	+/+	+/+	4100	5050	+/+	−/−	360
49	57 100	21	+/+	+/+	+/−	135	118	+/+	−/−	0
51	57 800	33 500	+/+	+/+	+/−	1600	0	+/−	−/−	470
11	71 500	14 700	+/+	−/+	+/−	2180	1865	+/+	−/−	100
2	79 000	4030	+/+	+/+	+/−	20	0	+/−	−/−	0
19	86 000	3400	+/+	+/+	+/−	69	297	+/−	−/−	12 000
47	92 700	16 600	+/+	+/+	+/+	354	6203	+/+	−/+	520
40	151 000	145 000	+/+	+/+	+/−	960	840	+/+	−/−	100
48	365 000	11 200	+/+	+/−	+/−	2320	320	+/−	+/−	3000
9	404 000	75 000	+/+	+/+	+/−	266	515	+/−	−/−	0
43	720 000	56 900	+/+	+/−	+/−	37 600	6440	+/+	−/−	2100

[a]ML: mucous layer.

[b]LP: lamina propria.

[c]PC: parietal cells.

fixed with 2% glutaraldehyde for 5 min on ice and incubated with peroxidase substrate (Histofine Simplestain DAB Solution). After several washes with PBS, sections were post-fixed with 0.5% OsO_4 for 60 min and washed again with PBS. After dehydration, sections were embedded in Epon. For flat embedding, gelatin capsules filled with Epon were positioned upside down exactly on the section areas that had been selected using parallel sections treated for IHC. After polymerization, the Epon blocks with tissue were peeled from the glass slides by heating. For precise trimming of the Epon blocks, small tissue areas ($1 \times 1\,mm^2$), which were readily identifiable under reflective light on the surfaces of the blocks, were selected. Ultrathin sections were cut on a Reichert Ultracut S (Leica Microsystems Heidelberg GmbH, Mannheim, Germany) and collected on Maxtaform grids (Pyser-SGL Ltd., Kent, UK). The sections were stained with lead citrate and examined using an H-7100 electron microscope (Hitachi High-Technologies Co., Tokyo, Japan).

Specificity of Anti-*H. pylori* Antibodies by ELISA and Western Blot

The specificity of the TMDU-mAb, Chemicon-mAb, and the DAKO-pAb was examined by ELISA and western blot with 3 strains of *H. pylori* used as the immunogen, 2 strains of other Helicobacters (*H. hepaticus* and *H. bilis*) and 10 strains of other control bacteria (*Campylobacter coli*, *C. jejuni, Vibrio parahaemolyticus*, *Escherichia coli*, *Salmonella enteritidis*, *Bacteroides fragilis*, *Staphylococcus epidermidis*, *Streptococcus sanguis*, *Mycobacterium tuberculosis*, and *Propionibacterium acnes*). Whole bacterial lysate was prepared from each bacterium by sonication on ice with an ultrasonic homogenizer (VP-5S ULTRA S homogenizer; Taitec, Koshigaya, Japan) twice at level 6 for 1 min. Lipopolysaccharide (LPS) was purified from the three strains of *H. pylori* with a kit (LPS Extraction Kit; iNtRON Biotechnology, Seongnam, Korea) according to the manufacturer's instructions.

ELISA was performed as follows. Flat-bottomed 96-well NUNC-immuno plates (Nalge Nunc International, Roskilde, Denmark) were coated with bacterial lysate (5 μg per well) in carbonate–bicarbonate buffer (pH 9.6) for 90 min at 37°C. The mAb or pAb was serially diluted in T-PBS and added to each well, and the plates were incubated for 90 min at 37°C. After incubation, they were incubated for 30 min further with biotinylated rabbit anti-mouse immunoglobulins (DAKO) or biotinylated swine anti-rabbit immunoglobulins (DAKO), and then for 30 min with horseradish peroxidase-conjugated streptavidin (DAKO), both at room temperature. Before and after each step, the plates were washed with T-PBS. After the reaction, citrate phosphate buffer (pH 5.4) containing 0.3% *o*-phenylenediamine dihydrochloride (Sigma-Aldrich Co.) and 0.012% H_2O_2 were added to each well, and the plates were incubated for 15 min at room temperature in the dark. The reaction was stopped by adding 25 μl of 2 M HCl to each well. The plates were read at 490 nm on Bio-Kinetics Reader (Bio-Tek Instruments Inc., VT, USA). Assay results were determined to be positive when a titration curve was unequivocally formed.

Western blot was performed as follows. Whole bacterial lysate and purified *H. pylori* LPS were separated by SDS-polyacrylamide gel electrophoresis using 12% polyacrylamide gel. All samples were transferred electrically to a polyvinylidene difluoride membrane with Mini Trans-Blot cell (Bio-Rad, Tokyo, Japan). Membranes were blocked overnight at 4°C with Block Ace (DS Pharma Biomedical Co. Ltd., Osaka, Japan). Membranes were then incubated for 90 min at room temperature with the appropriately diluted antibodies (TMDU-mAb 1:8000, Chemicon-mAb 1:2000, and DAKO-pAb 1:1000). Membranes were incubated for 30 min with biotinylated rabbit anti-mouse immunoglobulins (DAKO) or biotinylated swine anti-rabbit immunoglobulins (DAKO) and then for 30 min with horseradish peroxidase-conjugated streptavidin (DAKO), both at room temperature. Before and after each step, the membranes were washed in T-PBS. Finally, all blots were visualized by freshly prepared 1 M Tris-HCl (pH 7.5) containing 0.02% 3,3′-diaminobenzidine tetrahydrochloride (Sigma-Aldrich Co.) and 0.006% H_2O_2.

Real-Time PCR

Formalin-fixed paraffin-embedded tissue blocks were sliced 4 μm thick and placed in sterilized 1.5 ml centrifuge tubes. To prevent sample-to-sample contamination, a different microtome knife for each sample was used. The DNA of each section was extracted with a Dexpat kit (Takara Shuzo, Kyoto, Japan) according to the manufacturer's instructions. Bacterial DNA was extracted with a QIAamp for DNA Mini Kit (Qiagen, Hilden, Germany) according to the tissue protocol of the manufacturer's instructions. Real-time PCR was performed to amplify fragments of 16S ribosomal RNA of *H. pylori*. The primers used were HP-F, 5′-GGGCTTA GTCTCTCCAGTAATGCA-3′ and HP-R, 5′-GAGTTTTA ATCTTGCGACCGTACTC-3′, and the TaqMan probe was HP-P, 5′-CTAACGCATTAAGCATCCCGCCTGG-3′. The probe was labeled with 6-carboxyfluorescein on the 5′-end and 6-carboxytetramethylrhodamine (TAMRA) on the 3′-end. Real-time PCR mixtures contained 5 μl of template DNA, 100 nM concentrations of each primer, a 40 nM concentration of the probe, and Absolute QPCR ROX (500 nM) Mix (ABgene, Epsom, UK) in a total volume of 50 μl. Amplification and detection were performed with a detection system (ABI PRIZM 7900HT Sequence Detection System; Applied Biosystems, CA, USA) with the profile of 95°C for 5 min and then 50 cycles of 95°C for 15 s and 60°C for 1 min. The amount of bacterial DNA in the samples was estimated from internal standard samples of serially diluted bacterial DNA. The amount of bacterial DNA was expressed in terms of the number of bacterial genomes, with 1.25×10^{10} Da per genome used in the conversion. Negative controls without bacterial DNA were included in every PCR; background values were always less than one genome. Samples with one or more bacterial genome were considered to have positive

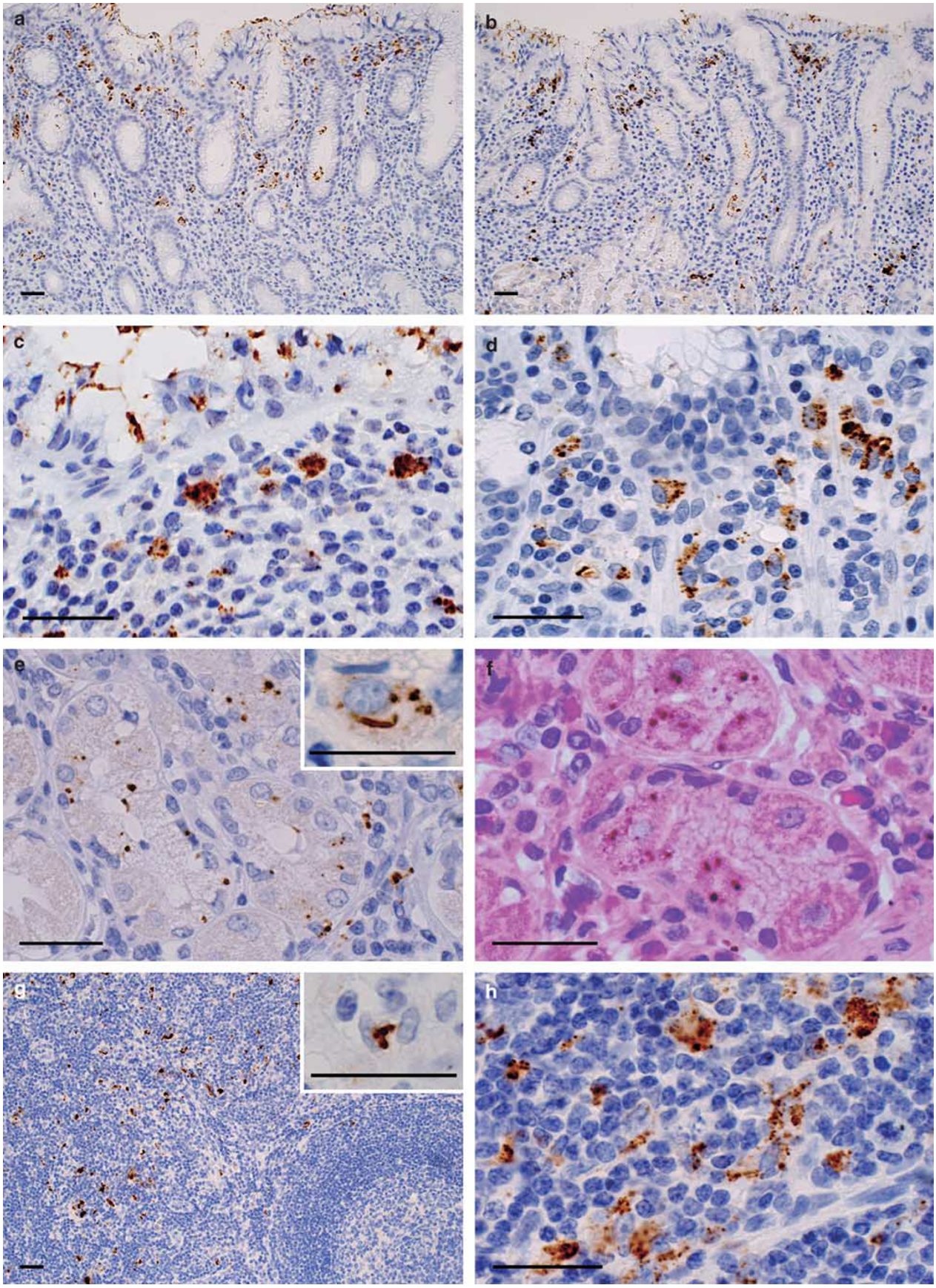
a
b
c
d
e
f
g
h

results. Total number of *H. pylori* in a single 4-μm-thick tissue section was obtained by multiplying the assay result by 40 times. The specificity of PCR for *H. pylori* was examined. Real-time PCR for *H. pylori* DNA was performed with quintuplicate samples of 10 pg DNA from each strain of bacteria, including *H. pylori*, *H. hepaticus*, and *H. bilis*, and other control bacteria as described before.

Grading of Gastritis

Formalin-fixed and paraffin-embedded tissue sections (4 μm thick) of the gastric corpus and antrum were stained with hematoxylin and eosin. Chronic inflammation, PMN neutrophil activity, glandular atrophy, intestinal metaplasia, and *H. pylori* density of the gastric mucosa were classified into four grades (0, absent; 1, mild; 2, moderate; and 3, marked) and overall results were evaluated by a single pathologist (DK) according to the updated Sydney System.[24]

Statistical Analyses

The frequency of samples with *H. pylori* detected by the Chemicon-mAb or the DAKO-pAb was compared with that detected by the TMDU-mAb using the exact McNemar's test. The strength of the independent relationships between the number of *H. pylori* genomes detected by PCR (dependent variable) and the IHC results for each location (independent variables) was expressed as the multivariate Spearman's rank correlation coefficient (r), where the independent variables were selected by the STEPWISE procedure with a P-value less than 0.10 for entry and removal; the statistical adjustment was also carried out for the potential confounding effects of clinicopathologic characteristics (Table 1) selected by the STEPWISE procedure. Such analyses were repeated to examine the independent relationships between the histologic grades by the Sydney System (dependent variable) and the mucosal density or location of *H. pylori* (independent variables); and between the results from the lymph nodes (dependent variable) and the mucosal density or location of *H. pylori* (independent variables). The STEPWISE multiple logistic regression analysis was also performed for binary dependent variables using standard methods, but the results were essentially comparable with those by the multivariate Spearman's rank correlation analysis and therefore only the results of the multivariate Spearman's rank correlation analysis are shown. A two-sided P-value less than 0.05 was considered statistically significant. All analyses were performed using the SAS statistical package (version 9.1; SAS Institute, NC, USA).

RESULTS

Specificity of the Methods for Detecting *H. pylori*

The specificity of the methods is shown in Table 2. PCR for *H. pylori* detected all strains of *H. pylori* with minimum cross-reactivity with other Helicobacters and no cross-reactivity with the control bacteria. The TMDU-mAb and Chemicon-mAb reacted with all strains of *H. pylori* and no cross-reactivity was found with the other Helicobacters and the control bacteria. The DAKO-pAb cross-reacted with *H. hepaticus*. The TMDU-mAb recognized an *H. pylori*-specific epitope of the LPS commonly shared by all three strains of this bacterium (Figure 1). The Chemicon-mAb and DAKO-pAb did not react with the LPS, but reacted with at least one protein on the membrane with the whole bacterial lysate.

Detection of *H. pylori* by Real-Time PCR, IHC, and Culture

Results of PCR in samples from the gastric corpus and antrum and from the two groups of gastric lymph nodes (nos. 3 and 4d) are shown in Table 3. *H. pylori* was not detected in the stomach or lymph nodes from five patients (nos. 29, 31, 32, 36, and 46). In the remaining 46 patients, *H. pylori* was detected in samples from the corpus of all patients, from the antrum of 38 (79%) patients, from the no. 3 lymph nodes of 34 (74%) patients, and from the no. 4d lymph nodes of 28 (61%) patients. In the *H. pylori*-positive patients, the median number of *H. pylori* per tissue section was 5420 (25th, 75th percentile: 1160, 28 200) in samples from the corpus, 3400 (678, 17 900) in samples from the antrum, 253 (123, 2030) in samples from the no. 3 lymph nodes, and 678 (275, 1990) in samples from the no. 4d lymph nodes.

The results of *H. pylori* detection by IHC with the TMDU-mAb in tissue sections from the stomach and lymph nodes are shown in Table 3. In the five patients in whom PCR failed to detect *H. pylori* in the stomach, IHC also failed to detect the bacterium in any location of the stomach or lymph nodes. In the 46 *H. pylori*-positive patients, the bacterium was found not only in the mucous layer but also in cells scattered in the lamina propria and in the parietal cells, in both the corpus and antrum (Figure 2). In the lymph nodes,

Figure 2 IHC with the TMDU-mAb of the stomach and gastric lymph nodes. Clusters of cells with intracellular *H. pylori* were widely distributed within the lamina propria, and were especially abundant just below the superficial epithelial cell layer of the antrum (**a**) and corpus (**b**). Higher magnification shows multiple round and various-sized immunoreactive particles in cells within the lamina propria of the antrum (**c**) and corpus (**d**). Several immunoreactive particles or rods (inset) were found in epithelial cells of the fundic glands (**e**). Hematoxylin counterstaining with intensified eosin shows that the immunoreactive particles in the fundic glands (the color changed a little) are located in the parietal cells (**f**). In the lymph nodes, *H. pylori*-positive cells were clustered at the paracortical area (**g**) and were morphologically similar to those found in the lamina propria (**h**). *H. pylori*-positive cells were rarely observed in the lymphatic sinus and a few cells with several immunoreactive round particles (**g**, inset) were found in the four samples from *H. pylori*-positive patients. Bars = 30 μm.

Table 4 Results of IHC with the *H. pylori*-specific antibodies in each location of the stomach and lymph nodes from the 46 *H. pylori*-positive subjects

Location of *H. pylori*	Number (%) of samples with *H. pylori* detected by IHC with		
	TMDU-mAb	Chemicon-mAb	DAKO-pAb
Gastric corpus			
Mucous layer	40 (87)	33 (72)*	35 (76)
Lamina propria	37 (80)	0 (0)**	6 (13)**
Parietal cells	19 (41)	5 (11)**	7 (15)*
Gastric antrum			
Mucous layer	24 (52)	20 (43)	21 (46)
Lamina propria	24 (52)	0 (0)**	4 (9)**
Parietal cells	4 (9)	0 (0)	1 (2)
Lymph nodes (no. 3)			
Paracortical area	24 (52)	0 (0)**	2 (4)**
Lymphatic sinus	2 (4)	0 (0)	0 (0)
Lymph nodes (no. 4d)			
Paracortical area	17 (37)	0 (0)**	2 (4)**
Lymphatic sinus	2 (4)	0 (0)	0 (0)

*$P<0.05$, **$P<0.001$ for comparing with TMDU-mAb by exact McNemar's test.

the bacterium was found in cells scattered in the paracortical area and rarely in the lymphatic sinus. Detection frequencies of *H. pylori* by IHC with the TMDU-mAb are shown in Table 4, and are compared with those by IHC with the Chemicon-mAb or the DAKO-pAb. The detection was most clear and frequent with the TMDU-mAb (Figure 3). Using TMDU-mAb, *H. pylori* was detected in the mucous layer, lamina propria, and parietal cells of the corpus and/or antrum from 40 (87%), 39 (85%), and 21 (46%) of the *H. pylori*-positive patients, respectively. *H. pylori* was found in the paracortical area of the nos. 3 and 4d lymph nodes from 24 (52%) and 17 (37%) of such patients, respectively, but rarely in the lymphatic sinus.

The results of culture for *H. pylori* from a fresh lymph node taken from the no. 3 lymph nodes before gastrectomy during surgery are shown in Table 3. Culture of samples from all *H. pylori*-negative patients was unsuccessful. The culture was successful in samples from 21 (46%) of the *H. pylori*-positive patients. The median quantity of *H. pylori* was 380 (250, 1200) (CFU/g).

Correlation between the Results by PCR and IHC

The correlation between the PCR and IHC results from the 46 *H. pylori*-positive patients was examined by multivariate analysis (Table 5). In the corpus, positive IHC of the mucous layer and the parietal cells independently correlated with the PCR results ($r=0.55$ and 0.62, respectively). In the antrum, positive IHC of the mucous layer correlated with the PCR results (0.78). Positive IHC of nos. 3 and 4d lymph nodes correlated with the PCR results (0.75 and 0.74, respectively). In the eight patients with negative PCR of the antrum, IHC was not positive in any location of the antrum or in any group of lymph nodes (Table 3). PCR was positive in all lymph node samples with positive IHC. Positive PCR but negative IHC was found in 10 and 11 samples from nos. 3 and 4d lymph nodes, respectively. These results indicate that IHC was specific, but less sensitive than PCR.

Mucosal Density or Location of *H. pylori* and Grades of the Sydney System

The correlation between the PCR or IHC results and the grades of the Sydney System was examined by multivariate analysis (Table 6). The gastric PCR results (mucosal density of *H. pylori*) correlated with PMN infiltration of the corpus ($r=0.53$) and antrum (0.46), and with chronic inflammation of the antrum (0.56), whereas they inversely correlated with corpus glandular atrophy (−0.42) and intestinal metaplasia of the corpus (−0.39) and antrum (−0.32). Positive IHC of the lamina propria independently correlated with chronic

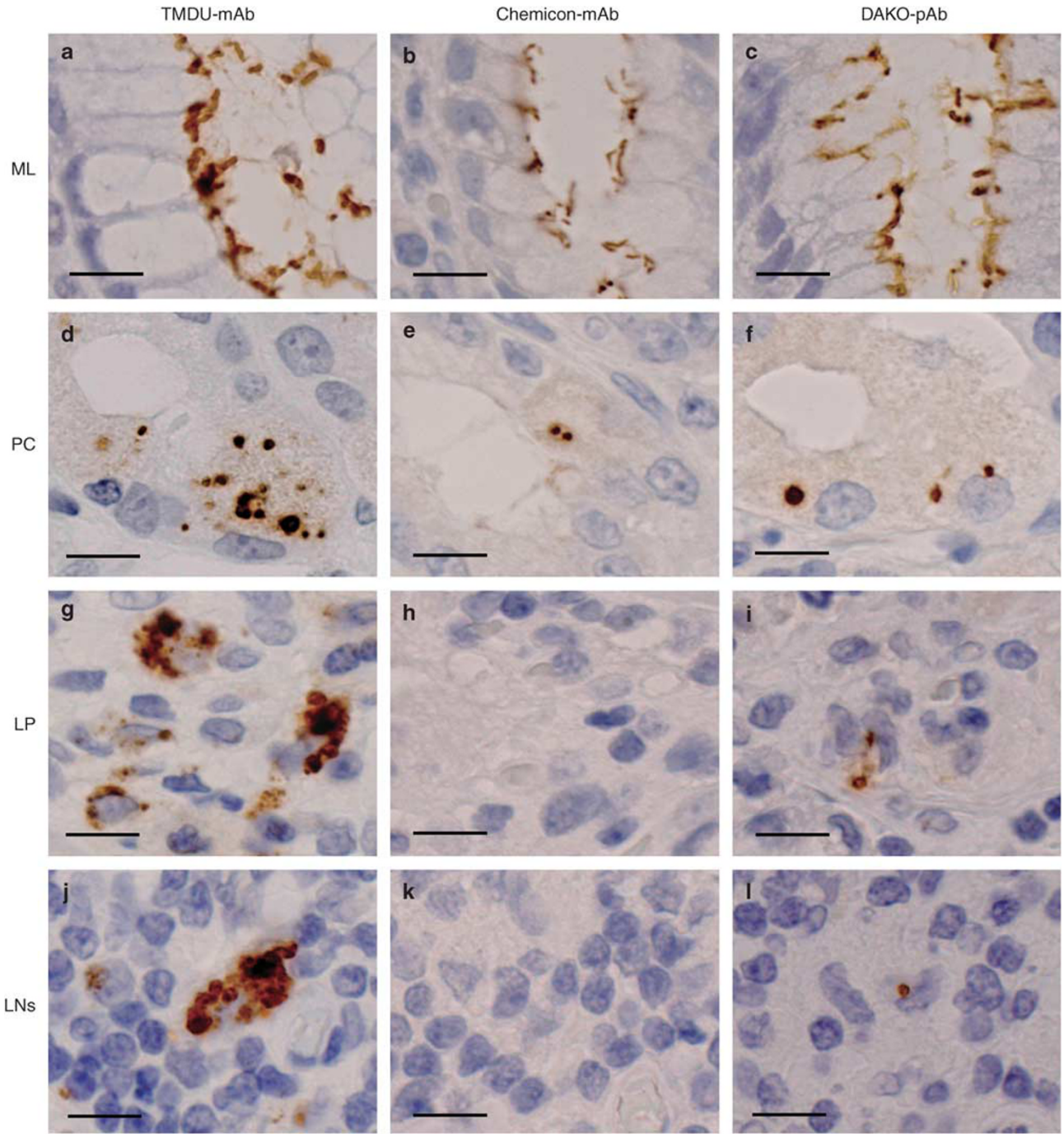

Figure 3 Comparison of the IHC results with the three anti-*H. pylori* antibodies. Representative IHC results with the TMDU-mAb (left column), the Chemicon-mAb (middle column), and DAKO-pAb (right column) are compared in the mucous layer (ML, upper row), in the parietal cells (PC, second row), in the lamina propria (LP, third row) of the stomach, and at the paracortical area of the gastric lymph nodes (LNs, lower row), respectively. Although the detection frequency and staining intensity were different, the immunoreactive *H. pylori* was not different morphologically among these antibodies when they were detected in the mucous layer (**a**–**c**) or in the parietal cells (**d**–**f**). There were remarkable differences in the IHC results for intracellular *H. pylori* in the lamina propria (**g**–**i**) or in the lymph nodes (**j**–**l**). Many intracellular round particles were found with the TMDU-mAb (**g**, **j**), a few particles with the DAKO-pAb (**i**, **l**), and no reactivity with the Chemicon-mAb (**h**, **k**). Bars = 10 μm.

inflammation of the corpus (0.43) and antrum (0.61). Corpus glandular atrophy was inversely correlated with positive IHC of the lamina propria (−0.32) and parietal cells (−0.65). Intestinal metaplasia was inversely correlated with positive IHC of the gastric mucosa (−0.31 to −0.43). The *H. pylori* density grade correlated not only with positive IHC of the mucous layer of the corpus (0.37) and antrum (0.84), but also with positive IHC of the corpus parietal cells (0.51).

Table 5 Correlation between the PCR and IHC results

IHC in each location	*n*	PCR	
		Median	*r* (*P*)[a]
Corpus			
Mucous layer			
+	40	9830	
−	6	520	0.55 (<0.001)
Lamina propria			
+	37	7550	NS[b]
−	9	1800	
Parietal cells			
+	19	57 100	
−	27	3000	0.62 (<0.001)
Model R^2			0.57
Antrum			
Mucous layer			
+	24	15 500	0.78 (<0.001)
−	22	144	
Lamina propria			
+	24	8380	NS
−	22	245	
Parietal cells			
+	4	13 800	NS
−	42	890	
Model R^2			0.63
Lymph nodes			
No. 3			
+	24	482	0.75 (<0.001)
−	22	0	
Model R^2			0.60
No. 4d			
+	17	1300	0.74 (<0.001)
−	29	0	
Model R^2			0.61

[a]Multivariate Spearman's rank correlation coefficient (*r*) of the PCR results (dependent variable) with the IHC results (independent variables) selected by the STEPWISE procedure. The analyses were performed separately for the corpus, antrum, no. 3 lymph nodes, and no. 4d lymph nodes. The correlation coefficients were also adjusted for clinicopathologic profiles selected from those in Table 1 by the STEPWISE procedure. The model R^2 included the effects of clinicopathologic profiles. For IHC variables, '+' was coded as 1 and '−' as 0.
[b]NS: not selected.

Correlation between the Results from the Stomach and the Gastric Lymph Nodes

Correlation between the results from the stomach and the gastric lymph nodes was examined by multivariate analysis (Table 7). The gastric PCR results (mucosal density of *H. pylori*) correlated with the *H. pylori* status of the gastric lymph nodes, including the PCR results (0.58–0.72), culture results (0.34–0.40), and positive IHC (0.46–0.65). In the antrum, but not in the corpus, positive IHC of the mucous layer correlated with the PCR results (no. 3: 0.42 and no. 4d: 0.57) and culture results (0.57) of the lymph nodes. Positive IHC of the lamina propria independently correlated with positive IHC of the lymph nodes (no. 3: 0.30 and no. 4d: 0.38).

Phenotypes of *H. pylori*-Positive Cells

In all five samples from the stomach, all of the *H. pylori*-positive cells in the lamina propria were stained with anti-CD68 mAb, but not with anti-fascin mAb and anti-MPO pAb (Figure 4). *H. pylori*-positive cells stained with the anti-MPO antibody were observed in the surface mucous layer or in the spaces between epithelial cells, but not in the lamina propria. In all five samples from the lymph nodes, most of the *H. pylori*-positive cells were stained with anti-CD68 mAb, but a few such cells were stained with the anti-fascin mAb.

Immunoelectron Microscopy

Although detailed observation of the tissue structures was not possible in many samples examined because of the use of paraffin sections, localization of the immunoreactive deposits was identified in some samples. *H. pylori* in the mucous layer showed dense rim staining of a whole *H. pylori* organism and the staining result was consistent with the supposed distribution of bacterial LPS. The same rim staining was also found in the immunoreactive particles or rods in the parietal cells. In the *H. pylori*-positive cells located in the lamina propria and lymph nodes, the signals were found in phagosome- or megasome-like structures, and most of the bacteria found in these cells appeared to be degraded, showing immunoreactive materials varying in size, shape, and density.

DISCUSSION

In *H. pylori*-positive patients, *H. pylori* was captured by macrophages in the lamina propria of the stomach in 85% of the patients and in the paracortical areas of the gastric lymph nodes in 63% of the patients. The bacterial DNA was found in the lymph nodes of 80% of the patients. Culture for *H. pylori* from the lymph nodes was successful in 46% of the patients. These results suggest that *H. pylori* invades the gastric mucosa and translocates to the draining lymph nodes.

Successful culture for *H. pylori* from the gastric lymph nodes provides evidence of bacterial translocation to the gastric lymph nodes. Contamination from the stomach is unlikely because the fresh lymph nodes for culture were obtained before gastrectomy during surgery. Bacterial

Table 6 Correlation between the PCR or IHC results of the stomach and the histologic grades by the Sydney System

Sydney System	Corpus								Antrum							
		PCR	IHC							PCR	IHC					
			ML[a]		LP[b]		PC[c]				ML		LP		PC	
	n	Median	+	−	+	−	+	−	*n*	Median	+	−	+	−	+	−
			n								*n*					
Chronic inflammation																
0	1	0	0	1	0	1	0	1	3	0	0	3	0	3	0	3
1	7	178	3	4	3	4	1	6	15	0	3	12	2	13	1	14
2	23	14 400	21	2	17	6	12	11	24	1740	14	10	14	10	1	23
3	20	4260	16	4	17	3	6	14	9	4130	7	2	8	1	2	7
r[d]		NS[e]		NS		0.43		NS		0.56		NS		0.61		NS
(P)[d]						(0.003)				(<0.001)				(<0.001)		
Model R^2		0.13						0.30		0.38						0.38
PMN infiltration																
0	3	605	2	1	2	1	0	3	7	0	0	7	1	6	0	7
1	21	1520	14	7	13	8	5	16	27	815	10	17	11	16	3	24
2	17	4780	14	3	14	3	7	10	15	11 200	13	2	11	4	1	14
3	10	64 300	10	0	8	2	7	3	2	8130	1	1	1	1	0	2
r[d]		0.53		NS		NS		0.39		0.46		0.50		NS		NS
(P)		(<0.001)						(0.006)		(0.001)		(<0.001)				
Model R^2		0.44						0.33		0.35						0.34
Glandular atrophy																
0	4	20 200	4	0	4	0	2	2	1	21	1	0	1	0	0	1
1	8	31 800	7	1	7	1	7	1	16	161	4	12	5	11	0	16
2	20	9830	15	5	15	5	9	11	13	19 200	11	2	9	4	2	11
3	19	1040	14	5	11	8	1	18	21	815	8	13	9	12	2	19
r[d]		−0.42		NS		−0.32		−0.65		NS		NS		NS		NS
(P)		(0.002)				(0.033)		(<0.001)								
Model R^2		0.17						0.59		0.12						0.12
Intestinal metaplasia																
0	18	21 100	17	1	14	4	10	8	15	16 200	10	5	11	4	2	13
1	14	1040	11	3	12	2	6	8	10	1120	3	7	4	6	0	10
2	13	4230	10	3	9	4	3	10	11	815	6	5	6	5	1	10
3	6	989	2	4	2	4	0	6	15	360	5	10	3	12	1	14
r[d]		−0.39		−0.31		NS		−0.35		−0.32		NS		−0.43		NS
(P)		(0.006)		(0.034)				(0.019)		(0.025)				(0.002)		
Model R^2		0.34						0.41		0.18						0.26
H. pylori *density*																
0	19	605	11	8	9	10	0	19	26	16	2	24	5	21	0	26
1	12	1790	9	3	10	2	6	6	10	2450	7	3	6	4	1	9
2	9	29 000	9	0	8	1	5	4	8	12 950	8	0	7	1	0	8
3	11	79 000	11	0	10	1	8	3	7	86 000	7	0	6	1	3	4
r[d]		0.82		0.37		NS		0.51		0.87		0.84		NS		NS
(P)		(<0.001)		(0.008)				(<0.001)		(<0.001)		(<0.001)				
Model R^2		0.71						0.46		0.80						0.74

[a]ML: mucous layer.

[b]LP: lamina propria.

[c]PC: parietal cells.

[d]Multivariate Spearman's rank correlation coefficient (r) of the histologic grades (dependent variables) with the PCR or IHC results (independent variables) selected by the STEPWISE procedure. The analyses were performed separately for corpus PCR, corpus IHC, antrum PCR, and antrum IHC. The correlation coefficients were also adjusted for clinicopathologic profiles selected from those in Table 1 by the STEPWISE procedure. The model R^2 included the effects of clinicopathologic profiles. For IHC variables, '+' was coded as 1 and '−' as 0.

[e]NS: not selected.

Table 7 Correlation between the results from the stomach and the gastric lymph nodes

Results from the stomach	*n*	Results from the lymph nodes						
		PCR		Culture (CFU/g)	IHC			
					No. 3		No. 4d	
		No. 3	No. 4d		+	−	+	−
Corpus PCR								
Median	51				26 200	775	23 400	1810
r[a]		0.66	0.58	0.34		0.65		0.46
(*P*)[a]		(<0.001)	(<0.001)	(0.017)		(<0.001)		(0.001)
Model R^2		0.49	0.51	0.25		0.43		0.45
Antrum PCR								
Median	51				4900	59	14 700	294
r		0.72	0.68	0.40		0.54		0.51
(*P*)		(<0.001)	(<0.001)	(0.005)		(<0.001)		(<0.001)
Model R^2		0.57	0.68	0.28		0.29		0.49
Corpus IHC		Median			*n*			
Mucous layer								
+	40	208	240	0	22	18	16	24
−	11	0	0	0	2	9	1	10
r (*P*)		NS[b]	NS	NS		NS		NS
Lamina propria								
+	37	205	200	0	20	17	14	23
−	14	0	0	0	4	10	3	11
r (*P*)		NS	NS	NS		NS		NS
Parietal cells								
+	19	215	297	100	12	7	10	9
−	32	48	0	0	12	20	7	25
r (*P*)		NS	NS	NS		NS		NS
Antrum IHC								
Mucous layer								
+	24	369	853	205	16	8	14	10
−	27	24	0	0	8	19	3	24
r		0.42	0.57	0.57		NS		NS
(*P*)		(0.004)	(<0.001)	(<0.001)				
Lamina propria								
+	24	253	678	100	16	8	14	10
−	27	24	0	0	8	19	3	24
r		NS	NS	NS		0.30		0.38
(*P*)						(0.041)		(0.007)
Parietal cells								
+	4	2230	4270	320	4	0	4	0
−	47	73	30	0	20	27	13	34
r (*P*)		NS	NS	NS		NS		NS
Model R^2		0.27	0.62	0.40		0.14		0.46

[a]Multivariate Spearman's rank correlation coefficient (*r*) of the PCR, culture, or IHC results of the lymph node (dependent variables) with the PCR or IHC results of the corpus and antrum (independent variables) selected by the STEPWISE procedure. The analyses were performed separately for corpus PCR, antrum PCR, and IHC of the corpus and antrum. The correlation coefficients were also adjusted for clinicopathologic profiles selected from those in Table 1 by the STEPWISE procedure. The model R^2 included the effects of clinicopathologic profiles. For IHC variables, '+' was coded as 1 and '−' as 0.

[b]NS: not selected.

translocation occurs frequently in humans.[25] Some believe that bacterial translocation may be a normal event, rather than a disease process, that is necessary to allow the gut-associated lymphoid tissue to generate immunocompetent cells.[26] In patients with gastric cancer, the normal mucosal barrier of the stomach may be disrupted by malignant tissue, but in the present study, positive culture was not correlated with the clinicopathologic data, including ulceration of the tumor and lymph node metastasis (data not shown). Because the *H. pylori* effector molecule VacA causes massive vacuolar degeneration of the epithelial cells, thus disrupting the gastric epithelial barrier, it is likely that translocation occurs in *H. pylori*-infected persons even without gastric cancer.

Successful detection of intracellular *H. pylori* was achieved by the novel anti-*H. pylori* mAb that was made for the current study. During hybridoma screening, we searched for *H. pylori*-specific antibodies that bound to the bacteria in the gastric lymph nodes because we had cultured *H. pylori* from the gastric lymph nodes before the screening. Detection sensitivity of the novel *H. pylori*-specific mAb (TMDU-mAb) for extracellular *H. pylori* was not significantly different from that of the commercially available anti-*H. pylori* antibodies used for comparison. There was a remarkable difference in the sensitivity for detecting intracellular *H. pylori*, which may have been due to differences in the antigens recognized by each antibody. The TMDU-mAb reacted with LPS, whereas the other antibodies reacted with a protein or proteins. LPS may be more resistant than proteins to intracellular digestion of phagocytes.

The presence of *H. pylori*-positive cells within the lamina propria from *H. pylori*-infected patients strongly suggests that *H. pylori* invades the gastric mucosa. *H. pylori* invasion into the lamina propria has been reported by several investigators. Andersen and Holck[16] reported that small amounts of immunopositive material were observed subepithelially in the lamina propria in biopsies from 13 of 34 *H. pylori*-infected patients. They used antibodies to *H. pylori* that were raised in rabbits by intravenous immunization of boiled bacteria. Mai *et al*[17] identified *H. pylori* cellular components in the lamina propria of antral biopsy specimens from *H. pylori*-infected patients. They used polyclonal rabbit antibodies to *H. pylori* whole bacteria and the 61 kDa subunit of *H. pylori* urease. Ko *et al*[19] found a few bacteria within the cytoplasm of a macrophage in the lamina propria using immunoelectron microscopy with the DAKO-pAb. Necchi *et al*[20] recently reported that *H. pylori* was detected inside cytoplasm of epithelial cells, in intraepithelial intercellular spaces, and in underlying lamina propria using immunoelectron microscopy with the six different antibodies, including the DAKO-pAb, directed against bacterial lysates, purified VacA, or purified CagA. The specification sheet of the DAKO-pAb describes that the antibody was prepared according to the original method by Andersen and Holck.[16] Many other investigators[27–31] also used the DAKO-pAb to show the usefulness of IHC for detecting extracellular *H. pylori* on the gastric mucosal surface, especially after eradication therapy. They did not comment about the detection of the bacterium in the lamina propria, however, probably because the immunoreactive signals were weak and infrequent, as shown in the present study.

All of the *H. pylori*-positive cells in the lamina propria and many such cells in the lymph nodes were stained with the anti-CD68 antibody (clone KP1), but not with the anti-fascin and anti-MPO antibodies. Only a few such cells in the lymph nodes were stained with the anti-fascin antibody. Anti-CD68 antibodies such as EBM11[32] react not only with macrophages but also with dendritic cells, but the KP1 antibody is reported to not react with dendritic cells.[33] Fascin is strongly expressed in interdigitating dendritic cells at the paracortical areas of the lymph nodes.[34] Thus, the results suggest that *H. pylori*-positive cells in the lamina propria are macrophages that have captured the bacterium and migrated, in other words translocated, from the stomach to the T-cell zones of the lymph nodes where active immune response occurs. A few *H. pylori*-positive dendritic cells in the lymph nodes suggest that a minority of *H. pylori*-positive monocytes in the lamina propria may carry the phagocytosed bacteria to the lymph nodes and differentiate into dendritic cells.[35]

The presence of *H. pylori* captured by macrophages in the lamina propria correlated with the histologic grade of chronic inflammation in the gastric corpus and antrum. The correlation suggests that the *H. pylori*-positive macrophages may contribute to the induction and maintenance of chronic inflammation within the *H. pylori*-infected gastric mucosa. The presence of *H. pylori* in the gastric mucosa is associated with strong IL-12 production[36] and the presence of large numbers of Th1 cells.[37] Differentiation of naive T cells into activated Th1 cells requires the presence of IL-12, which is predominantly produced by macrophages rather than epithelial cells. Thus, it is likely that the *H. pylori*-positive macrophages within the lamina propria contribute to the accumulation of *H. pylori*-specific $CD4^+$ T cells by the strong IL-12 production of these macrophages. It is more likely that *H. pylori* was captured by subepithelial macrophages after invasion through the eroded or disrupted mucosal layer caused by *H. pylori*-induced epithelial cell damage. Indeed, *H. pylori*-positive macrophages were frequently clustered just beneath the epithelial cell layer. Further, IHC studies to locate the *H. pylori*-positive macrophages together with other immunocompetent cells or epithelial cells in identical histologic sections may allow us to test the hypothesis.

Whether *H. pylori* captured by macrophages is viable is not known. Several studies indicate that, although effectively ingested by professional phagocytes, *H. pylori* is more resistant to phagocytic killing than other Gram-negative bacteria.[38] *In vitro* studies demonstrate that phagocytosis of type I *H. pylori* by macrophages is delayed and that viable bacteria accumulate in larger than normal phagosomes, referred to as megasomes, which result from homotypic phagosome

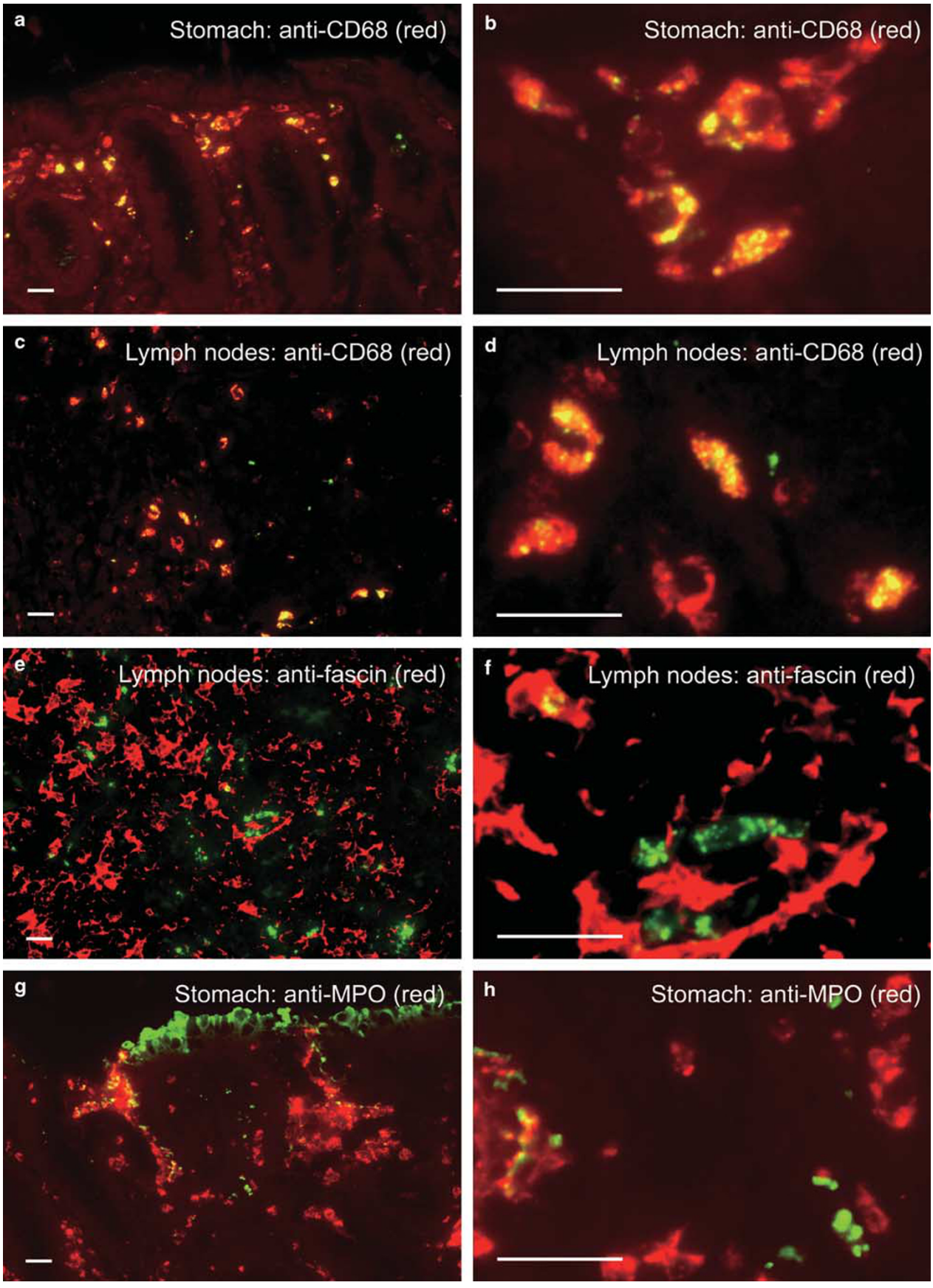
a
Stomach: anti-CD68 (red)
b
Stomach: anti-CD68 (red)
c
Lymph nodes: anti-CD68 (red)
d
Lymph nodes: anti-CD68 (red)
e
Lymph nodes: anti-fascin (red)
f
Lymph nodes: anti-fascin (red)
g
Stomach: anti-MPO (red)
h
Stomach: anti-MPO (red)

fusion.[39] Subsequent macrophage apoptosis might enable the escape of the bacteria.[40] In the present study, immunoreactive signals were found in megasome-like structures, but they seemed to be degraded because the signals were diffusely distributed and did not show the rim staining that is typical of whole bacteria, as observed for the extracellular *H. pylori* in the mucous layer. Alternatively, some of the immunoreactive round particles captured by macrophages may represent coccoid forms of *H. pylori*. Coccoid *H. pylori* maintains the same antigenic characteristics as the bacillary form.[41] In addition, experimental animal models indicate that the coccoid form of *H. pylori* reverts to the bacillary form and induces gastritis and ulcer.[42] Successful culture of *H. pylori* from the gastric lymph nodes suggests that some of *H. pylori*-positive macrophages at the paracortical areas may have carried coccoid forms of *H. pylori*. Wells *et al*[43] suggested that intestinal macrophages have a key role in transporting intestinal bacteria into the mesenteric lymph nodes. *H. pylori*-positive macrophages may contribute to transport the bacterium into the gastric lymph nodes. The close correlation between the *H. pylori*-positive cells in the lamina propria and the gastric lymph nodes also suggests the migration of such cells from the stomach to the lymph nodes. These macrophages carrying intracellular *H. pylori* might stimulate the adaptive immune response to the bacterium more intensely and efficiently in the lymph nodes than do the cells in the gastric mucosa.

Gastric mucosal density of *H. pylori* correlated with the grade of PMN cell infiltration rather than chronic inflammation. The bacterial density may reflect the number of bacteria attached to epithelial cells that cause PMN cell infiltration. The gastric mucosal density also correlated with the numbers of *H. pylori* by PCR or culture as well as with positive IHC in the lymph nodes. Dense colonization of *H. pylori* may damage the epithelial barrier more frequently and allows more bacteria, or more bacterial components including DNA, to enter the lamina propria and translocate to the lymph nodes directly without uptake by phagocytes or indirectly after capture by macrophages in the lamina propria.

In the antrum, but not in the corpus, the presence of *H. pylori* in the mucous layer correlated with the gastric mucosal density, and thus with the *H. pylori* status of the lymph nodes. The correlations confined to the antrum seemed to be associated with the status of intestinal metaplasia that was predominant in the gastric antrum. *H. pylori* is rarely observed on the gastric mucosa with intestinal metaplasia.[44] Bacterial translocation may be decreased in the stomach with advanced intestinal metaplasia. Such effect of intestinal metaplasia on *H. pylori* colonization was also reflected by the inverse correlation of gastric mucosal density with intestinal metaplasia. Similarly, glandular atrophy of the corpus contributed to the decreased mucosal density as well as the decreased frequency of *H. pylori* in the parietal cells.

On the basis of sensitivities of PCR and culture, the failure of PCR to detect *H. pylori* from five samples of the no. 3 lymph nodes with positive culture requires explanation. For culture, a single lymph node was sampled from no. 3 lymph nodes during surgery. After surgery, a paraffin block of the no. 3 lymph nodes that included all nodes along the lesser curvature except for the cultured lymph node was prepared and used for PCR. The lack of a strong correlation between the culture and PCR results may have been caused by the different samples used for each assay. Indeed, *H. pylori*-positive macrophages were observed in a few of the no. 3 lymph nodes from *H. pylori*-positive patients.

The presence of large spiral-shaped Helicobacter organisms within the cytoplasm of parietal cells is a common finding in several animal species, such as rhesus monkeys,[45] cynomolgus monkeys,[46] rats,[47] cats, and dogs.[48] Electron microscopic observation indicates that these organisms in those animals reside within dilated intracellular canaliculi of parietal cells.[49] The existence of *H. pylori* in the parietal cell canaliculi in humans has also been reported.[14,50,51] The results of an ultrastructural quantitative study reported by Taniguchi *et al*[52] indicated that there was nearly one *H. pylori* per 100 parietal cells, and all of the *H. pylori* in the canaliculi appeared intact. Using immunoelectron microscopy, we found *H. pylori* in the parietal cell canaliculi that were morphologically similar to those found deep in the glands or in the mucous layer. These bacteria appeared intact, as evidenced by the rim staining of the immunoreactive particles, which is consistent with the LPS distribution of a whole *H. pylori* organism in the mucous layer. Furthermore, the presence of *H. pylori* in the corpus parietal cells correlated with gastric mucosal density as well as the grade of *H. pylori* density. *H. pylori* in the parietal cells may not be true intracytoplasmic invasion into epithelial cells, because the intracellular canaliculi continue to the lumen deep in the

Figure 4 Immunofluorescence double staining for phenotyping the *H. pylori*-positive cells in the lamina propria and gastric lymph nodes. The corpus (**a**, **b**, **g**, **h**) of the stomach from patient no. 47 and the no. 3 lymph nodes (**c**–**f**) from patient no. 48 are shown. Green signals (fluorescein isothiocyanate (FITC)): anti-*H. pylori* antibody (TMDU-mAb); red signals (tetramethylrhodamine isothiocyanate (TRITC)): anti-CD68 antibody (**a**–**d**), anti-fascin antibody (**e**, **f**), and anti-MPO antibody (**g**, **h**). Results of the double staining are merged in all pictures. The right column (**b**, **d**, **f**, **h**) shows higher magnification of the left column (**a**, **c**, **e**, **g**), respectively. In the stomach, all of the *H. pylori* signals in the lamina propria overlapped (yellow) with CD68-positive cells, whereas *H. pylori* signals are green in the surface mucous layer (**a**). Many yellow-colored round particles are clearly shown in the higher magnification (**b**). Similarly, in the lymph nodes, many of *H. pylori* signals were found in the CD68-positive cells but a few signals were not (**c**, **d**). The CD68-negative *H. pylori* signals in the lymph nodes were fascin positive (**e**, **f**). *H. pylori* signals were never observed in the MPO-positive neutrophils in the lamina propria, but many *H. pylori*-positive neutrophils were observed in the surface mucous layer or in the spaces between epithelial cells (**g**, **h**). Bars = 20 μm.

glands. Even by IHC with the TMDU-mAb, intracellular invasion into gastric epithelial cells was not identified, apart from the pseudoinvasion into parietal cells. Although the physiologic significance of *H. pylori* in the parietal cell canaliculi is not yet clear, several reports demonstrate that *H. pylori* infection is responsible for alterations in gastric physiology.[53]

The findings of the present study indicate that *H. pylori* does invade the gastric mucosa and translocates to the gastric lymph nodes. The observation of many *H. pylori* captured by macrophages in the lamina propria as well as in the lymph nodes suggests that *H. pylori*-specific T cells can be primed and maintained within these regions. On the basis of a recent animal study, Nagai *et al*[54] suggested that Peyer's patches have a critical role in priming $CD4^+$ T cells and that *H. pylori* is captured by dendritic cells in Peyer's patches or mesenteric lymph nodes where dendritic cells migrate after capturing antigens. Dendritic cells degrade proteins inefficiently, thus preserving the antigenic information contained in peptides. Macrophages are equipped to eliminate pathogens efficiently because of their high degradative phagosomal capacity, but under certain conditions, they can also process antigens to stimulate T cells.[55] As the exposure of immunocompetent cells to the bacterial antigens is far larger in the stomach than in the terminal ileum, it seems likely that *H. pylori*-positive macrophages in the lamina propria have more critical roles in priming T cells than do *H. pylori*-positive dendritic cells in Peyer's patches. Moreover, frequent translocation of *H. pylori* and/or *H. pylori*-carrying macrophages to the gastric lymph nodes may chronically stimulate the immune system, which then continuously provides *H. pylori*-specific T cells to the lamina propria. Chronic stimulation of the immune system may also lead some predisposed patients to various extra-gastric diseases associated with *H. pylori* infection.[56] Future studies are required to elucidate the immunologic and pathologic contributions of these *H. pylori*-positive macrophages in the lamina propria and gastric lymph nodes.

ACKNOWLEDGEMENT

We thank Ms Aya Miwa, Ms Manami Takizawa, Ms Kana Minegishi, Ms Pariko Yorozu, Ms Makiko Takahashi, and Ms Eri Uchino for their technical assistance. This study was supported by Japan Society for the Promotion of Science Grant-in-Aid for Scientific Research 16790203 (DK) and 18390112 (YE).

1. Makola D, Peura DA, Crowe SE. *Helicobacter pylori* infection and related gastrointestinal diseases. J Clin Gastroenterol 2007;41:548–558.
2. Dooley CP, Cohen H, Fitzgibbons PL, *et al*. Prevalence of *Helicobacter pylori* infection and histologic gastritis in asymptomatic persons. N Engl J Med 1989;321:1562–1566.
3. Kusters JG, van Vliet AH, Kuipers EJ. Pathogenesis of *Helicobacter pylori* infection. Clin Microbiol Rev 2006;19:449–490.
4. Marshall B. *Helicobacter pylori*: 20 years on. Clin Med 2002;2:147–152.
5. Baldari CT, Lanzavecchia A, Telford JL. Immune subversion by *Helicobacter pylori*. Trends Immunol 2005;26:199–207.
6. Yamaoka Y, Kita M, Kodama T, *et al. Helicobacter pylori cagA* gene and expression of cytokine messenger RNA in gastric mucosa. Gastroenterology 1996;110:1744–1752.
7. Reyrat JM, Pelicic V, Papini E, *et al*. Towards deciphering the *Helicobacter pylori* cytotoxin. Mol Microbiol 1999;34:197–204.
8. Mohammadi M, Czinn S, Redline R, *et al*. Helicobacter-specific cell-mediated immune responses display a predominant Th1 phenotype and promote a delayed-type hypersensitivity response in the stomachs of mice. J Immunol 1996;156:4729–4738.
9. D'Elios MM, Manghetti M, De Carli M, *et al*. T helper 1 effector cells specific for *Helicobacter pylori* in the gastric antrum of patients with peptic ulcer disease. J Immunol 1997;158:962–967.
10. Lundgren A, Trollmo C, Edebo A, *et al. Helicobacter pylori*-specific CD4+ T cells home to and accumulate in the human *Helicobacter pylori*-infected gastric mucosa. Infect Immun 2005;73:5612–5619.
11. Suerbaum S, Michetti P. *Helicobacter pylori* infection. N Engl J Med 2002;347:1175–1186.
12. Hazell SL, Lee A, Brady L, *et al*. Campylobacter pyloridis and gastritis: association with intercellular spaces and adaptation to an environment of mucus as important factors in colonization of the gastric epithelium. J Infect Dis 1986;153:658–663.
13. Bode G, Malfertheiner P, Ditschuneit H. Pathogenetic implications of ultrastructural findings in *Campylobacter pylori* related gastroduodenal disease. Scand J Gastroenterol Suppl 1988;142:25–39.
14. Tricottet V, Bruneval P, Vire O, *et al*. Campylobacter-like organisms and surface epithelium abnormalities in active, chronic gastritis in humans: an ultrastructural study. Ultrastruct Pathol 1986;10:113–122.
15. Price AB. Histological aspects of *Campylobacter pylori* colonisation and infection of gastric and duodenal mucosa. Scand J Gastroenterol Suppl 1988;142:21–24.
16. Andersen LP, Holck S. Possible evidence of invasiveness of *Helicobacter* (*Campylobacter*) *pylori*. Eur J Clin Microbiol Infect Dis 1990;9:135–138.
17. Mai UE, Perez-Perez GI, Allen JB, *et al*. Surface proteins from *Helicobacter pylori* exhibit chemotactic activity for human leukocytes and are present in gastric mucosa. J Exp Med 1992;175: 517–525.
18. Morozov IA. Possibility of *Helicobacter pylori* invasion into the lamina propria of the gastric mucosa. Arkh Patol 1994;56:19–22.
19. Ko GH, Kang SM, Kim YK, *et al*. Invasiveness of *Helicobacter pylori* into human gastric mucosa. Helicobacter 1999;4:77–81.
20. Necchi V, Candusso ME, Tava F, *et al*. Intracellular, intercellular, and stromal invasion of gastric mucosa, preneoplastic lesions, and cancer by *Helicobacter pylori*. Gastroenterology 2007;132:1009–1023.
21. Hamilton SR, Aaltonen LA. Pathology and Genetics of Tumours of the Digestive System. IARC Press: Lyon, 2000.
22. Japanese Research Society for Gastric Cancer. Japanese Classification of Gastric Carcinoma. Kanehara & Co.: Tokyo, 1995.
23. Harlow E, Lane D. Antibodies: a Laboratory Manual. Cold Spring Harbor Laboratory Press: New York, 1988.
24. Dixon MF, Genta RM, Yardley JH, *et al*. Classification and grading of gastritis. The updated Sydney System. International Workshop on the Histopathology of Gastritis, Houston 1994. Am J Surg Pathol 1996; 20:1161–1181.
25. O'Boyle CJ, MacFie J, Mitchell CJ, *et al*. Microbiology of bacterial translocation in humans. Gut 1998;42:29–35.
26. Wells CL, Maddaus MA, Simmons RL. Proposed mechanisms for the translocation of intestinal bacteria. Rev Infect Dis 1988;10:958–979.
27. Jonkers D, Stobberingh E, de Bruine A, *et al*. Evaluation of immunohistochemistry for the detection of *Helicobacter pylori* in gastric mucosal biopsies. J Infect 1997;35:149–154.
28. Marzio L, Angelucci D, Grossi L, *et al*. Anti-*Helicobacter pylori* specific antibody immunohistochemistry improves the diagnostic accuracy of *Helicobacter pylori* in biopsy specimen from patients treated with triple therapy. Am J Gastroenterol 1998;93:223–226.
29. Toulaymat M, Marconi S, Garb J, *et al*. Endoscopic biopsy pathology of *Helicobacter pylori* gastritis. Comparison of bacterial detection by immunohistochemistry and Genta stain. Arch Pathol Lab Med 1999; 123:778–781.
30. Eshun JK, Black DD, Casteel HB, *et al*. Comparison of immunohistochemistry and silver stain for the diagnosis of pediatric *Helicobacter pylori* infection in urease-negative gastric biopsies. Pediatr Dev Pathol 2001;4:82–88.
31. Ishihara S, Okuyama T, Ishimura N, *et al*. Intragastric distribution of *Helicobacter pylori* during short-term omeprazole therapy: study using Carnoy's fixation and immunohistochemistry for detection of bacteria. Aliment Pharmacol Ther 2001;15:1485–1491.

32. Kelly PM, Bliss E, Morton JA, *et al.* Monoclonal antibody EBM/11: high cellular specificity for human macrophages. J Clin Pathol 1988;41: 510–515.
33. Pulford KA, Rigney EM, Micklem KJ, *et al.* KP1: a new monoclonal antibody that detects a monocyte/macrophage associated antigen in routinely processed tissue sections. J Clin Pathol 1989;42: 414–421.
34. Pinkus GS, Pinkus JL, Langhoff E, *et al.* Fascin, a sensitive new marker for Reed–Sternberg cells of Hodgkin's disease. Evidence for a dendritic or B cell derivation? Am J Pathol 1997;150:543–562.
35. Randolph GJ, Inaba K, Robbiani DF, *et al.* Differentiation of phagocytic monocytes into lymph node dendritic cells *in vivo*. Immunity 1999;11:753–761.
36. Karttunen RA, Karttunen TJ, Yousfi MM, *et al.* Expression of mRNA for interferon-gamma, interleukin-10, and interleukin-12 (p40) in normal gastric mucosa and in mucosa infected with *Helicobacter pylori*. Scand J Gastroenterol 1997;32:22–27.
37. Meyer F, Wilson KT, James SP. Modulation of innate cytokine responses by products of *Helicobacter pylori*. Infect Immun 2000;68: 6265–6272.
38. Allen LA. The role of the neutrophil and phagocytosis in infection caused by *Helicobacter pylori*. Curr Opin Infect Dis 2001;14:273–277.
39. Allen LA, Schlesinger LS, Kang B. Virulent strains of *Helicobacter pylori* demonstrate delayed phagocytosis and stimulate homotypic phagosome fusion in macrophages. J Exp Med 2000;191:115–128.
40. Chaturvedi R, Cheng Y, Asim M, *et al.* Induction of polyamine oxidase 1 by *Helicobacter pylori* causes macrophage apoptosis by hydrogen peroxide release and mitochondrial membrane depolarization. J Biol Chem 2004;279:40161–40173.
41. Chan WY, Hui PK, Leung KM, *et al.* Coccoid forms of *Helicobacter pylori* in the human stomach. Am J Clin Pathol 1994;102:503–507.
42. Cellini L, Allocati N, Angelucci D, *et al.* Coccoid *Helicobacter pylori* not culturable *in vitro* reverts in mice. Microbiol Immunol 1994;38:843–850.
43. Wells CL, Maddaus MA, Simmons RL. Role of the macrophage in the translocation of intestinal bacteria. Arch Surg 1987;122:48–53.
44. Testoni P, Colombo E, Scelsi R, *et al.* Tissue staining for *Helicobacter pylori* in intestinal metaplasia: correlation with its extension and histochemical subtypes. Ital J Gastroenterol 1995;27:285–290.
45. Dubois A, Tarnawski A, Newell DG, *et al.* Gastric injury and invasion of parietal cells by spiral bacteria in rhesus monkeys. Are gastritis and hyperchlorhydria infectious diseases? Gastroenterology 1991;100: 884–891.
46. Reindel JF, Fitzgerald AL, Breider MA, *et al.* An epizootic of lymphoplasmacytic gastritis attributed to *Helicobacter pylori* infection in cynomolgus monkeys (*Macaca fascicularis*). Vet Pathol 1999;36: 1–13.
47. Giusti AM, Crippa L, Bellini O, *et al.* Gastric spiral bacteria in wild rats from Italy. J Wildl Dis 1998;34:168–172.
48. Hermanns W, Kregel K, Breuer W, *et al.* Helicobacter-like organisms: histopathological examination of gastric biopsies from dogs and cats. J Comp Pathol 1995;112:307–318.
49. Geyer C, Colbatzky F, Lechner J, *et al.* Occurrence of spiral-shaped bacteria in gastric biopsies of dogs and cats. Vet Rec 1993;133:18–19.
50. Chen XG, Correa P, Offerhaus J, *et al.* Ultrastructure of the gastric mucosa harboring Campylobacter-like organisms. Am J Clin Pathol 1986;86:575–582.
51. Rollason TP, Stone J, Rhodes JM. Spiral organisms in endoscopic biopsies of the human stomach. J Clin Pathol 1984;37:23–26.
52. Taniguchi Y, Kimura K, Satoh K, *et al. Helicobacter pylori* detected deep in gastric glands: an ultrastructural quantitative study. J Clin Gastroenterol 1995;21(Suppl 1):S169–S173.
53. Moss S, Calam J. *Helicobacter pylori* and peptic ulcers: the present position. Gut 1992;33:289–292.
54. Nagai S, Mimuro H, Yamada T, *et al.* Role of Peyer's patches in the induction of *Helicobacter pylori*-induced gastritis. Proc Natl Acad Sci USA 2007;104:8971–8976.
55. Savina A, Amigorena S. Phagocytosis and antigen presentation in dendritic cells. Immunol Rev 2007;219:143–156.
56. Franceschi F, Gasbarrini A. *Helicobacter pylori* and extragastric diseases. Best Pract Res Clin Gastroenterol 2007;21:325–334.